NANO LETTERS

Letter

pubs.acs.org/NanoLett

Electrically Tunable van der Waals Interaction in Graphene−Molecule Complex

Manoharan Muruganathan,*[,†] Jian Sun,[†] Tomonori Imamura,[†] and Hiroshi Mizuta[†,‡]

[†]School of Materials Science, Japan Advanced Institute of Science and Technology, Nomi 923-1211, Japan

[‡]Nanoelectronics and Nanotechnologies Research Group, Faculty of Physical Sciences and Engineering, University of Southampton, Highfield, Southampton SO17 1BJ, U.K.

Supporting Information

ABSTRACT: van der Waals (vdW) interactions play a central role in the surface-related physics and chemistry. Tuning of the correlated charge fluctuation in a vdW complex is a plausible way of modulating the molecules interaction at the atomic surface. Here, we report the vdW interaction tunability of the graphene−CO_2 complex by combining the first-principles calculations with the vdW density functionals and the time evaluation measurements of CO_2 molecules adsorption/desorption on graphene under an external electric field. The field-dependent charge transfer within the complex unveils the controllable tuning of CO_2 from acceptor to donor. Meanwhile, the configuration of the adsorbed molecule, the equilibrium distance from graphene and O−C−O bonding angle, is modified accordingly. The range of electrical tunability is a unique feature for each type of molecule.

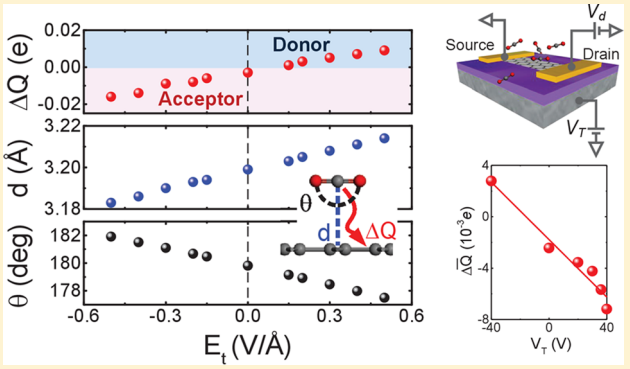

KEYWORDS: *van der Waals complex, electrical tunability of vdW interaction, graphene−molecule vdW complexes, field-dependent charge transfer*

van der Waals (vdW) interactions are the decisive factor in molecular physisorption on a surface,[1−3] adhesion between micromachined surfaces in micro- and nanomechanical devices,[4] friction in tribology discipline,[5] and the characteristics of vdW heterostructures.[6,7] Currently, surface modification, i.e., tailoring or replacing the original materials, is a commonly employed method to selectively create specific vdW complexes for their favorable properties.[8−10] The London dispersion forces involved in a vdW complex of molecules adsorbed on a surface are electro-dynamically correlated to the charge transfer inside the complex. This raises the possibility of tuning such vdW interaction electrically, e.g., by applying an external electrical field, which offers easy access to the desired features while keeping the original materials untouched.[11−13] The difficulty of characterizing vdW complexes impedes the direct observation. Here, we demonstrate the electrical tunability of the vdW interactions for graphene−molecule complexes with first-principles calculations combined with the experimental study of the electrically controlled charge transfer for the graphene−CO_2 vdW complex. Graphene is strongly modulated by the vdW interactions with physisorbed molecules upon its transport properties. Owing to the high-quality crystal lattice along with its 2D structure, graphene exhibits an extremely suppressed electrical noise, making the possibility to measure weak fluctuations in its transport properties. The inaccessible interaction is therefore transferred into an easily measurable electric signal.[14,15] The transport measurements verify the tunability of vdW interactions between graphene and CO_2 molecules from the varied charge transfer from molecules to graphene under external fields.

First, the first-principles calculations are utilized to understand the interaction between graphene and a CO_2 molecule adsorbed on it. All the first-principles calculations were performed with the SIESTA package.[16] van der Waals exchange correlation density functionals were used (vdW-DF)[17,18] as implemented by Roman-Perez.[19] Norm-conserving pseudopotentials of Troullier and Martins[20] were used and pseudoatomic orbitals energy shift was kept at 1 mRy. The integration grids in real space had 400 Ry maximum kinetic energy cutoff. Double-ζ plus polarization basis sets were used in these calculations. Each of the simulated systems under investigation consisted of a 25 Å × 14.766 Å × 17.0503 Å graphene−molecule rectangular supercell (96 carbon atoms and molecules) with a single molecule adsorbed in the central region of the *YZ* plane. These dimensions make sure that the distance between adjacent graphene layers is greater than 10 Å. The *k*-point was set to 1 × 5 × 5 for the Brillouin zone integration. In the case of density of states calculations a separate finer set of *k*-points 1 × 9 × 9

Received: September 10, 2015
Revised: November 11, 2015
Published: November 12, 2015

DOI: 10.1021/acs.nanolett.5b03653
Nano Lett. 2015, 15, 8176−8180

were used. Initially, with the same supercell and *k*-point samplings, the configurations of the graphene−molecular systems were optimized by fully relaxing the atomic structures until the remaining residual force smaller than 0.01 eV/Å. Adsorption energy calculations are first performed to find out the optimum distance between the gas molecule and the graphene. The adsorption energy is defined as $E_{Ad} = E_{(mol-gra)} - (E_{gra}+E_{mol})$ where $E_{mol-gra}$ is the total energy of the graphene with a molecule adsorption and E_{gra} and E_{mol} are the total energies of the graphene and the isolated CO_2 molecule, respectively.

The potential energy surface scans show that the adsorbed CO_2 molecule lies most stably in the direction perpendicular to the carbon−carbon bond of the graphene hexagon, sitting at an equilibrium distance of 3.3 Å with adsorption energy of 202 meV (see Supporting Information Figure S9). Basis set superposition error and dipole corrections are accounted in these calculations. Additionally, the equilibrium distance and adsorption energy are calculated to be 3.3 Å and 193 meV, respectively, with vdW functional vdW-DF-cx,[21] showing a good agreement with the vdW-DF results. The low adsorption energy reflects a weak interaction between the CO_2 molecule and the graphene and its physisorption nature. This is also revealed by the density of states (DOS) calculations[22−24] as the electronic states of CO_2 are superimposed on to these of the graphene (Figure 1a). The weak interaction of the highest occupied molecular orbital (HOMO) of CO_2 (the peak shown at −9.31159 eV in Figure 1a) with the graphene states results in a small bonding−antibonding splitting of 11.92 meV (Figure 1b). The three-dimensional plots of the wave functions visually elucidate these abstract features. Figure 1c depicts the bonding wave function at −9.60327 eV showing a weak graphene−CO_2 orbital overlap, while a repulsion is noted in its antibonding wave function at −9.59135 eV, as shown in Figure 1d. Furthermore, these interacting CO_2 states are still located energetically far below the Fermi level, clarifying the weak charge transfer within the graphene−CO_2 complex. Consequently, the vdW interaction plays a dominant factor in the graphene−CO_2 complex interaction.

Now, we unveil the electrical tunability of the graphene−CO_2 molecule vdW complex by carrying out first-principles calculations with Mulliken population analysis.[25] The vdW complex is investigated under an external electric field, E_t, applied perpendicularly to graphene. In practice, the electric field is usually introduced to the graphene surface by applying a voltage, V_T, to the substrate. A finite element simulation is first employed to estimate the strength of electric field generated with the application of V_T, which shows that an E_t of −0.15 V/Å (0.15 V/Å) is achieved on the graphene surface for a V_T of 40 V (−40 V) (Figure 2a and Supporting Information Figure S5). It is worth to mention that the high voltage of 40 V is not necessary to access to this electric field strength at graphene surface. For instance, a substrate with thinner oxide or the local gated technique can effectively reduce the gate voltage. The charge transfer from the CO_2 molecule to graphene, ΔQ, is calculated with varying E_t. Figure 2b plots the calculated charge transfer as a function of electric field. Without applying a tuning field, the CO_2 molecule acts as a weak acceptor to graphene, receiving 0.003*e* charge. The varied ΔQ is noted as E_t is introduced, disclosing the nature of tunable charge transfer in the vdW complex. In particular, the CO_2 molecules switch their role to donor in the field of 0.15 V/Å (Figure 2b). The switched polarity of the graphene−CO_2 molecule complex

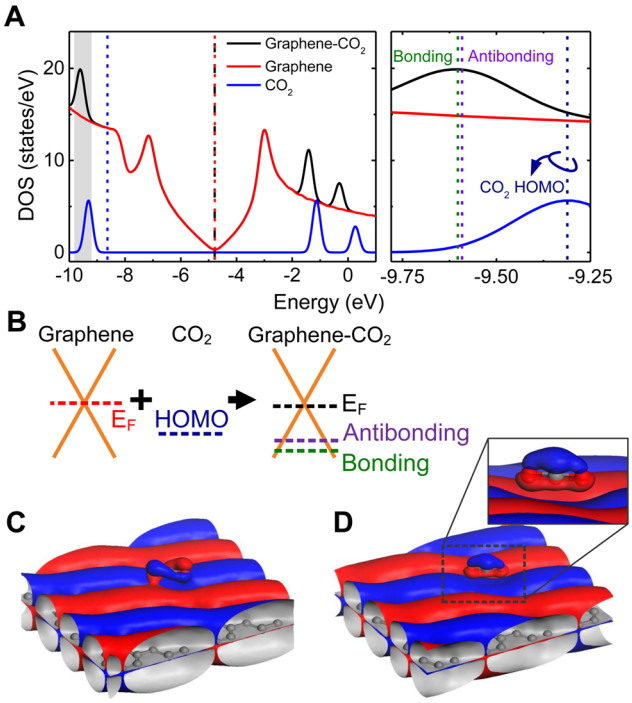

Figure 1. Density of states and wave functions of a graphene−CO_2 complex. (a) DOS plots of graphene−CO_2 complex, graphene, and CO_2 molecule. Vertical dash-lines locate their Fermi levels at −4.7840, − 4.7788, and −8.6309 eV, respectively. The right panel is the zoomed-in details of the gray region (Gaussian broadening energy in DOS plots: 0.2 eV). (b) Schematic of the bonding−antibonding splitting in graphene−CO_2 complex. Due to the weak interaction nature of graphene−CO_2 complex, CO_2 HOMO level at −9.31159 eV (4.53279 eV below graphene Fermi level) interacts with continuous DOS spectrum of graphene and forms bonding and antibonding states with a small splitting of 11.92 meV. (c,d) Bonding (−9.60327 eV) and antibonding (−9.59135 eV) Gamma point wave functions of graphene−CO_2 complex, respectively. Blue and red colors denote the positive and negative iso-surfaces, respectively (iso-value: 0.005 e/Å^3).

system under the electric fields is also exhibited as a change in the electric dipole moments (see Supporting Information Figures S10 and S11).

Fabrication started with the mechanical exfoliation of monolayer graphene from highly ordered pyrolytic graphite on to the silicon substrate covered by 300 nm thermally grown SiO_2. Then, graphene flakes were etched into desired bar-shapes by transferring the pattern from the E-beam lithography defined poly(methyl methacrylate) (PMMA) etching mask in oxygen plasma. In the end, electrodes were metallized with Ti/Au stack via conventional electron beam lithography, metal evaporation, and lift-off processes. After fabrication, hydrogen annealing at 400 °C was performed in an infrared lamp furnace in a mixed gas ambient of H_2/Ar (1:9) at atmospheric pressure (see Supporting Information Section 1 for more details). First, the device was thermally annealed at the pressure of 10^{-3} Pa in the probe-station at 200 °C for 2 h to remove surface adsorbates on graphene. The Ohmic contact between graphene and electrodes was confirmed by the linear current−voltage response measured at source and drain. In the CO_2 adsorption measurements, source−drain current in the graphene device was measured with a constant bias voltage V_D of 1 mV while fixed tuning voltage V_T was applied at back gate. Initially, CO_2 gas was injected at a flow rate of 150 sccm with a mass flow

DOI: 10.1021/acs.nanolett.5b03653
Nano Lett. 2015, 15, 8176−8180

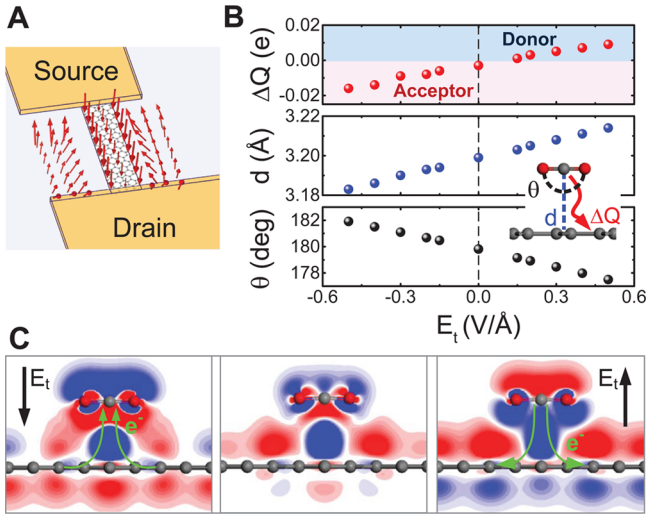

Figure 2. Electrical tuning of van der Waals bonding of CO_2 molecule to graphene. (a) Finite element simulation showing the direction of electric filed at the surface of 2 Å above graphene with 40 V applied back gate voltage. (b) First-principles calculations of charge transfer ΔQ, bonding distance d, and bending angle θ of the adsorbed CO_2 molecule on graphene at various tuning electric fields. Inset illustrates an absorbed molecule. (c) Charge density distributions in the cut planes across the CO_2 at varied electrical fields (tuning voltages). From left to right: − 0.15 V/Å (40 V), 0 V/Å (0 V), and 0.15 V/Å (−40 V). Blue color denotes electron density enrichment and red color shows depletion for the iso-values of ±0.0001 e/Å^3.

controller. After atmospheric pressure was reached in the chamber (~30 min), injection was stopped. At designated time points, the application of constant tuning voltage were interrupted; instead, a quick sweeping of gate voltage was performed from −40 to 40 V to extract the value of Dirac point from the gate modulation curve[26] (see Supporting Information Section 2). Immediately after the gate voltage sweep, tuning voltage was resumed. After the measurement at each tuning voltage, the chamber was evacuated and thermal annealing was employed to regenerate graphene.

The predicted tunable charge transfer in the vdW complex, if any, should be measured as varied doping concentration in graphene under the tuning electric fields. In order to prove the above theoretical findings, we measure the variations of doping concentrations, n_d, in graphene exposed to CO_2 molecules under various values of V_T. Figure 3a illustrates the schematic of the device and measurement configuration. The gate modulation measurements are carried out along with the time, from which the doping concentrations are extracted (Figure 3b). Thermal annealing at ~10^{-4} Pa is employed *in situ* to regenerate graphene by cleansing the adsorbates before each measurement.[15] For V_T ranging from 0 to 40 V, positive increases in the doping concentration n_d are observed, which indicate that the adsorbed CO_2 molecules act as acceptors. Interestingly, for a V_T of −40 V, a negative n_d is measured, signifying that the CO_2 molecules act as the donor. These results strongly substantiate the prediction of the first-principles calculations. The data also allows a rough estimation of the coverage of CO_2 molecules on graphene surface for each particular V_T, if the area occupied by a single adsorbed CO_2 molecule is known.

We can extract the value of the average charge transfer $\overline{\Delta Q}$ from Figure 3b with a simple dynamic model.[27] Then, the doping concentration is expressed as $n_d(t) = N(t)\ \overline{\Delta Q}$ where $N(t)$ represents the temporal density of CO_2 molecules adsorbed on graphene and is described by

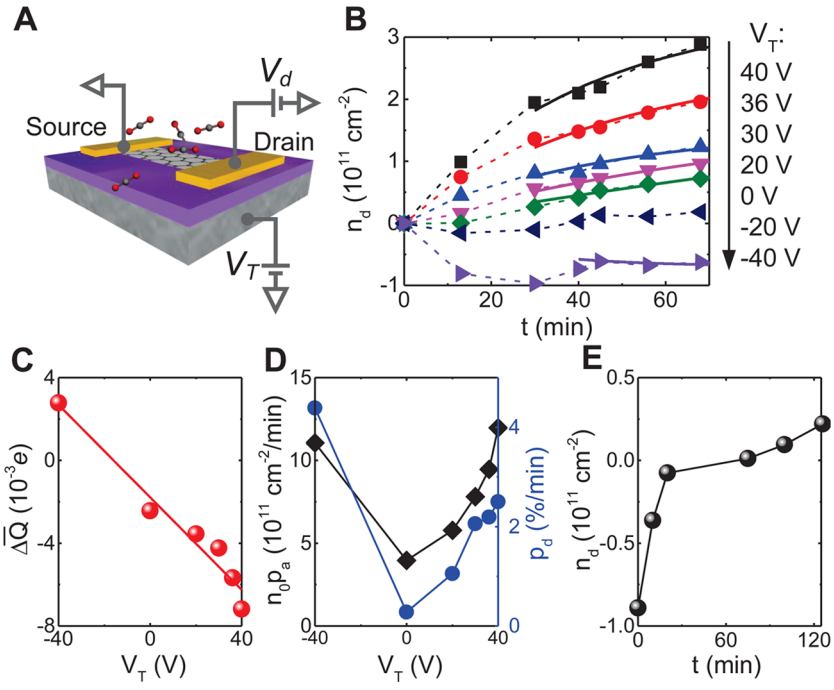

Figure 3. Measurements of CO_2 adsorptions at varied tuning voltages V_T. (a) Schematic of the measurement configuration. Tuning voltage, V_T, is applied at substrate. (b) Doping concentration at various tuning voltages, V_T, from 40 to −40 V. The positive/negative sign of n_d denotes hole/electron. The solid lines are the fits to eq 1. (c,d) Plot of the values of averaged charge transfer $\overline{\Delta Q}$, adsorption rate n_0p_a and desorption rate p_d, respectively. Solid line in (c) is a linear fit. (e) Change of doping concentration after tuning voltage switched from −40 to 40 V.

DOI: 10.1021/acs.nanolett.5b03653
Nano Lett. 2015, 15, 8176−8180

$$N(t) = \frac{n_0 p_a}{p_d}(1 - e^{-p_d t}) + N_0 \quad (1)$$

where n_0 is the density of the molecules in the gas phase (remains constant after gas injection is stopped), N_0 is the initial adsorption density on graphene, and p_a and p_d are the adsorption and desorption rates, respectively. By fitting eq 1 to the measured temporal change in the adsorption density, the values of $\overline{\Delta Q}$ are obtained for different V_T. Figure 3c clearly manifests the charge transfer tuned via applied external fields, showing a good agreement with the first-principles calculations prediction. In addition, the adsorption and desorption rates are also extracted from the data fittings (Figure 3d). The adsorption rate enhanced by the increased magnitude V_T, accelerates the adsorption process due to the polarizability of the CO_2 molecules. Hence, similar adsorption rates are read for V_T of −40 and 40 V. In contrast, the desorption rate at V_T of −40 V is approximately twice as high as that for V_T of 40 V, as a result of a weaker vdW interaction between CO_2 molecule and graphene at −40 V, reflecting a longer bonding distance and lower charge transfer (Figure 2b).

It is noted that the application of constant voltage V_T is shortly interrupted for an interval of ∼0.5 min at each individual data point in a series of temporal measurements. During the interval, V_T is swept from −40 to 40 V in order to obtain gate modulation curves for n_d extraction. Under these circumstances, the charge transfer from those previously adsorbed molecules is probably altered and molecules freshly adsorbed during the sweeping exhibit varied charge transfer different from that adsorbed under constant V_T. Here we carry out a measurement at an extreme condition to clarify that the interruption of constant V_T only slightly affects the analysis of n_d at constant V_T. Graphene is first kept at $V_T = -40$ V for 2 h; a n_d of -0.89×10^{11} cm^{-2} is measured (Figure 3e). V_T is then suddenly switched to 40 V; the positive shift of n_d with a relatively slow rate of -0.4×10^{10} cm^{-2}/min is observed. Hence, the short interruption of constant V_T only has a insignificant impact on the extraction of n_d for V_T. It also suggests that the electrical tuning plays an important role during the formation of graphene−CO_2 vdW bonding; that is to say once the complex formed, it is stable to some extent.

In order to clarify the tunable charge transfer, we visualize the two-dimensional charge density difference distributions in the graphene−CO_2 complex[28] in Figure 2c under the tuning field of −0.15 V/Å (left), zero (center), and 0.15 V/Å) (right) (see a detailed three-dimensional visualization as Supporting Video). Here, the charge density difference of CO_2 adsorption is defined by $\rho_{Ad} = \rho_{CO_2+Gra} - \rho_{CO_2} - \rho_{Gra}$, where ρ_{CO_2+Gra}, ρ_{Gra}, and ρ_{CO_2} are the charge densities of the graphene with adsorbed CO_2, the pristine graphene, and an isolated CO_2 molecule for a particular electric field, respectively. The tunability of the charge transfer can be understood by applying Lorentz force. For a zero tuning field, the vdW interaction governs the charge transfer between CO_2 and graphene, which can be seen from the induced dipole structure between them. As the tuning field is switched on, a strong electrostatic force induces a comparable order of charge redistribution inside the vdW complex; that is to say, the charge transfer is tuned electrically. Under positive (negative) tuning fields, more electrons are taken from (given to) the CO_2 molecule (see Supporting Video). The reversed dipole distribution are clearly seen for the negative and positive tuning fields (left and right of Figure 2c). This is associated with the change in other parameters for the graphene−CO_2 vdW interactions. Particularly, the vdW bonding distance, d, is changed from 3.199 Å at the natural state (without electric field) to 3.203 Å (3.194 Å) for E_T of 0.15 V/Å (−0.15 V/Å). The bonding angle between carbon and oxygen atoms also varies accordingly (Figure 2b and Supporting Information Figure S12).

We extend the present theoretical investigation to other graphene−molecule complexes (see Supporting Information Figures S13 and S14). In Table. 1, we compare the charge transfer ΔQ calculated for various vdW complexes at negative, zero, and positive tuning fields.[15,29,30] These results indicate that the individual complexes show different tunabilities. We would like to mention that the charge transfer and its tunability do not necessarily correlate with the molecule's polarizability as it is mainly dominated by the graphene−molecule vdW interaction. For instance, NH_3 molecule provides much lower doping to graphene than O_2; even it has a larger polarizability of 2.103 Å^3 than that of O_2 (1.45 Å^3).[31] It should also be noted that such a unique tunability does not depend on the initial condition of graphene. Thus, in addition to the conductivity change of graphene stemmed from the molecular adsorptions, a commonly employed gas sensing mechanism, the observation of the doping tunability may provide a new approach to gas molecule detection.

Table 1. Electrical Tunability of the Charge Transfer in Various Graphene−Molecule Complexes[a]

	ΔQ (e)		
molecule	−0.15 V/Å	0 V/Å	0.15 V/Å
CO_2	−0.006	−0.003	0.001
C_6H_6	0.009	0.019	0.029
CO	−0.003	0.001	0.004
NH_3	0.015	0.018	0.022
O_2	−0.242	−0.208	−0.174

[a]Negative and positive signs indicate the role of molecules as acceptor and donor, respectively.

With the complex of graphene and its physisorbed CO_2 molecules, we have discovered the tunability of the vdW interaction at external electric fields. The field-dependent charge transfer in CO_2−graphene complex was unveiled with associated changes in the equilibrium CO_2−graphene distance and the O−C−O bonding angle. By reversing the substrate bias polarity, the charge transfer direction also switched, signifying the role of physisorbed CO_2 molecules can be altered electrically between donor and acceptor. Our results entice us to attempt the possibility of recognizing the type of molecules adsorbed on graphene from the unique tunable charge transfer between them, which is applicable even to chemical molecules possessing very poor doping capability.

■ ASSOCIATED CONTENT

Supporting Information

The Supporting Information is available free of charge on the ACS Publications website at DOI: 10.1021/acs.nanolett.5b03653.

Device fabrication and characterization details; finite element simulation results; molecular adsorption dynamic model and ab initio calculations results (PDF)

Charge density difference (AVI)

DOI: 10.1021/acs.nanolett.5b03653
Nano Lett. 2015, 15, 8176−8180

AUTHOR INFORMATION

Corresponding Author

*E-mail: mano@jaist.ac.jp (M.M).

Notes

The authors declare no competing financial interest.

ACKNOWLEDGMENTS

This work was supported by Grant-in-Aid for Scientific Research (No. 25220904) from Japan Society for the Promotion of Science. The authors thank M. E. Schmidt and X. Wang for their helpful discussions.

REFERENCES

(1) Dzyaloshinskii, I. E.; Lifshitz, E. M.; Pitaevskii, L. P. *Sov. Phys. Uspekhi* **1961**, *4*, 153.
(2) Bartels, L. *Nat. Chem.* **2010**, *2*, 87−95.
(3) Aradhya, S. V.; Frei, M.; Hybertsen, M. S.; Venkataraman, L. *Nat. Mater.* **2012**, *11*, 872−876.
(4) DelRio, F. W.; de Boer, M. P.; Knapp, J. A.; David Reedy, E.; Clews, P. J.; Dunn, M. L. *Nat. Mater.* **2005**, *4*, 629−634.
(5) Krim. *Adv. Phys.* **2012**, *61*, 155−323.
(6) Geim, A. K.; Grigorieva, I. V. *Nature* **2013**, *499*, 419−425.
(7) Kushima, A.; Qian, X.; Zhao, P.; Zhang, S.; Li, J. *Nano Lett.* **2015**, *15*, 1302−1308.
(8) Lalatonne, Y.; Richardi, J.; Pileni, M. P. *Nat. Mater.* **2004**, *3*, 121−125.
(9) Lessel, M.; Loskill, P.; Hausen, F.; Gosvami, N. N.; Bennewitz, R.; Jacobs, K. *Phys. Rev. Lett.* **2013**, *111*, 111.
(10) Huttmann, F.; Martínez-Galera, A. J.; Caciuc, V.; Atodiresei, N.; Schumacher, S.; Standop, S.; Hamada, I.; Wehling, T. O.; Blügel, S.; Michely, T. ArXiv150902020 Cond-Mat, 2015.
(11) Müller-Dethlefs, K.; Hobza, P. *Chem. Rev.* **2000**, *100*, 143−168.
(12) Zhou, J.; Wang, Q.; Sun, Q.; Jena, P.; Chen, X. S. *Proc. Natl. Acad. Sci. U. S. A.* **2010**, *107*, 2801−2806.
(13) Foroutan-Nejad, C.; Marek, R. *Phys. Chem. Chem. Phys.* **2014**, *16*, 2508−2514.
(14) Novoselov, K. S. *Science* **2004**, *306*, 666−669.
(15) Schedin, F.; Geim, A. K.; Morozov, S. V.; Hill, E. W.; Blake, P.; Katsnelson, M. I.; Novoselov, K. S. *Nat. Mater.* **2007**, *6*, 652−655.
(16) Soler, J. M.; Artacho, E.; Gale, J. D.; García, A.; Junquera, J.; Ordejón, P.; Sánchez-Portal, D. *J. Phys.: Condens. Matter* **2002**, *14*, 2745.
(17) Dion, M.; Rydberg, H.; Schröder, E.; Langreth, D. C.; Lundqvist, B. I. *Phys. Rev. Lett.* **2004**, *92*, 92.
(18) Berland, K.; Cooper, V. R.; Lee, K.; Schröder, E.; Thonhauser, T.; Hyldgaard, P.; Lundqvist, B. I. *Rep. Prog. Phys.* **2015**, *78*, 066501.
(19) Román-Pérez, G.; Soler, J. M. *Phys. Rev. Lett.* **2009**, *103*, 096102.
(20) Troullier, N.; Martins, J. L. *Phys. Rev. B: Condens. Matter Mater. Phys.* **1991**, *43*, 1993−2006.
(21) Berland, K.; Hyldgaard, P. *Phys. Rev. B: Condens. Matter Mater. Phys.* **2014**, *89*, 035412.
(22) Bogani, L.; Wernsdorfer, W. *Nat. Mater.* **2008**, *7*, 179−186.
(23) Wiley: Principles of Adsorption and Reaction on Solid Surfaces - Richard I. Masel. http://as.wiley.com/WileyCDA/WileyTitle/productCd-0471303925.html (accessed Jun 3, 2015).
(24) Zhang, Y.-H.; Chen, Y.-B.; Zhou, K.-G.; Liu, C.-H.; Zeng, J.; Zhang, H.-L.; Peng, Y. *Nanotechnology* **2009**, *20*, 185504.
(25) Mulliken, R. S. *J. Chem. Phys.* **1955**, *23*, 1833−1840.
(26) Kim, S.; Nah, J.; Jo, I.; Shahrjerdi, D.; Colombo, L.; Yao, Z.; Tutuc, E.; Banerjee, S. K. *Appl. Phys. Lett.* **2009**, *94*, 062107.
(27) Chen, S.; Cai, W.; Chen, D.; Ren, Y.; Li, X.; Zhu, Y.; Kang, J.; Ruoff, R. S. *New J. Phys.* **2010**, *12*, 125011.
(28) Clark, S. J.; Segall, M. D.; Pickard, C. J.; Hasnip, P. J.; Probert, M. J.; Refson, K.; Payne, M. C. *Z. Kristallogr. - Cryst. Mater.* **2005**, *220*, 567−570.
(29) Chakarova-Käck, S. D.; Schröder, E.; Lundqvist, B. I.; Langreth, D. C. *Phys. Rev. Lett.* **2006**, *96*, 96.
(30) Sato, Y.; Takai, K.; Enoki, T. *Nano Lett.* **2011**, *11*, 3468−3475.
(31) CRC Handbook of Chemistry and Physics, 85th Edition. https://www.crcpress.com/CRC-Handbook-of-Chemistry-and-Physics-85th-Edition/Lide/9780849304859 (accessed Nov 12, 2015).

DOI: 10.1021/acs.nanolett.5b03653
Nano Lett. 2015, 15, 8176−8180